Ferromagnetic polarons in the one-dimensional ferromagnetic Kondo model with quantum mechanical $S=3/2$ core spins

Danilo R. Neuber,* Maria Daghofer, Hans Gerd Evertz, and Wolfgang von der Linden
Institute of Theoretical and Computational Physics, Graz University of Technology, Petersgasse 16, A-8010 Graz, Austria

Reinhard M. Noack
Fachbereich Physik, Philipps-Universität Marburg, D-35032 Marburg, Germany
(Received 12 January 2005; revised manuscript received 4 October 2005; published 3 January 2006)

We present an extensive numerical study of the ferromagnetic Kondo lattice model with quantum mechanical $S=3/2$ core spins. We treat one orbital per site in one dimension using the density-matrix renormalization group and include on-site Coulomb repulsion between the electrons. We examine parameters relevant to manganites, treating the range of low to intermediate doping, $0 \lesssim x < 0.5$. In particular, we investigate whether quantum fluctuations favor phase separation over the ferromagnetic polarons observed in a model with classical core spins. We obtain very good agreement of the quantum model with previous results for the classical model, finding separated polarons, which are repulsive at short distance for finite t_{2g} superexchange J'. Taking on-site Coulomb repulsion into account, we observe phase separation for small but finite superexchange J', whereas for larger J', polarons are favored in accordance with simple energy considerations previously applied to classical spins. We discuss the interpretation of compressibilities and present a phase diagram with respect to doping and the t_{2g} superexchange parameter J' with and without Coulomb repulsion.

DOI: 10.1103/PhysRevB.73.014401 PACS number(s): 75.47.Lx, 71.10.Fd, 71.38.−k

I. INTRODUCTION

The ferromagnetic Kondo lattice model has been widely used as a minimal model to describe some features of the manganites[1] $La_{1-x}Sr_xMnO_3$, $La_{1-x}Sr_{1+x}MnO_4$, and $La_{2-2x}Sr_{1+2x}Mn_2O_7$. The model contains one itinerant e_g orbital and the t_{2g} core spin at each site. The e_g electrons are ferromagnetically coupled to the $S=3/2$ core spins generated by the fully occupied t_{2g} orbitals. The large ferromagnetic Hund's rule coupling leads to the formation of two bands, the lower and upper Kondo bands, with the e_g electrons predominantly parallel to the core spins in the lower band. The core spins strongly influence the mobility of the e_g electrons via double exchange (DE). At high hole density, this leads to a ferromagnetic arrangement of the core spins, while antiferromagnetism is preferred for the completely filled lower Kondo band. In the opposite case of an empty Kondo band, the t_{2g} core spins are antiferromagnetically oriented due to superexchange.

Since the core spins have a fairly large spin, $S=3/2$, they are frequently approximated by classical spins, greatly simplifying calculations. Furthermore, the on-site Coulomb repulsion U between the e_g electrons is often neglected because double occupancy is already suppressed by the Hund's rule coupling and because its treatment considerably increases the numerical effort.[2] A review of these semiclassical simulations can be found in Refs. 3 and 4, and references therein. Several of these studies[5,6] have found that phase separation into regions with either ferromagnetically or antiferromagnetically aligned core spins occurs when the lower Kondo band is nearly empty ($n \gtrsim 0$) or nearly filled ($n \lesssim 1$).

In previous work by some of the current authors, also treating the core spins classically, similar numerical results were obtained.[2,7] However, a closer analysis of the data revealed that the features that had been interpreted by other authors to indicate phase separation (a discontinuity in the electron density versus the chemical potential, a pseudogap in the one-particle density of states) were, in fact, due to small, independent ferromagnetic polarons. Likewise, ferromagnetic polarons have been found for the almost empty lower Kondo band, for localized $S=1/2$ quantum spins.[8,9] For the antiferromagnetic Kondo model,[10] small ferromagnetic droplets were predicted by Kagan *et al.*[11] The question arises whether the correct quantum-mechanical treatment of the $S=3/2$ core spins would favor phase separation instead of independent ferromagnetic polarons, especially for $T=0$. In this paper, we address the influence of quantum spins on this issue.

The impact of a quantum-mechanical treatment of spins on models for the manganites has been addressed in Refs. 12–15. In one dimension, quantum-mechanical core spins with $S=1/2$ were employed in a number of studies conducted with the density-matrix renormalization group (DMRG).[8,9,16,17] Recently, Garcia *et al.*[18] presented a phase diagram for $S=1/2$, which, however, was determined for only three values of the density and did not address the physically interesting region of doping, $x<1/3$, treated in this paper. Quantum-mechanical spins with $S=3/2$ have been briefly addressed in an exploratory study.[6] The authors report phase separation when the lower Kondo band is nearly filled.

In this work, we present extensive calculations for the one-dimensional (1D) ferromagnetic Kondo lattice model with $S=3/2$ core spins using the DMRG. We observe that quantum spins yield results in very good agreement with previous calculations[2] for a model with classical core spins: for finite t_{2g} superexchange J', polarons are favored over phase separation. In addition, we include an on-site Coulomb

repulsion U between the e_g electrons: accordingly, the superexchange parameter J', which favors antiferromagnetic (AFM) alignment of the core spins, is renormalized and the effective antiferromagnetic coupling J_{eff} is weakened. This leads to an increased polaron size for large J' and phase separation for small J'.

The remainder of this paper is organized as follows. In Sec. II, we define the model Hamiltonian, for which we present DMRG results in Sec. III. We discuss the ground-state configurations in Sec. III A. In Sec. III A 1, we show that the polarons are actually repulsive at short distance. We then discuss the impact of the antiferromagnetic t_{2g} superexchange J' and of the Hubbard repulsion U and show that quantum-mechanical core spins are very well approximated by classical spins (Sec. III A 2). We discuss the transition to the homogeneous ferromagnetic chain in Sec. III A 3 and present a phase diagram in Sec. III B. Negative compressibility and the discontinuity in the density versus the chemical potential are often taken as a sign for phase separation. In Sec. III C, we argue that negative compressibility is an uncertain result when obtained from numerical methods such as the DMRG, quantum Monte Carlo, or exact diagonalization and show that a discontinuity in the density can equally well result from small independent polarons. Finally, Sec. IV summarizes and discusses the results presented in this work.

II. MODEL HAMILTONIAN AND METHOD

We study the ferromagnetic Kondo lattice model with localized quantum core spins $S=3/2$ and one orbital per site, including a small Heisenberg-like superexchange between the core spins as well as an on-site Coulomb repulsion U between the e_g electrons

$$\hat{H} = -\sum_{\langle ij\rangle,\sigma} t c_{i\sigma}^{\dagger} c_{j\sigma} + U\sum_i \hat{n}_{i,\uparrow}\hat{n}_{i,\downarrow} - J_H \sum_i \vec{s}_i \cdot \vec{S}_i + J' \sum_{\langle ij\rangle} \vec{S}_i \cdot \vec{S}_j, \tag{1}$$

where $c_{i\sigma}$ ($c_{i\sigma}^{\dagger}$) creates (destroys) an e_g electron with spin σ at site i, $\hat{n}_{i,\sigma}=c_{i\sigma}^{\dagger}c_{i\sigma}$ is the corresponding density operator, $\vec{S}_i$ is the core spin at site i, and $\vec{s}_i$ the electron spin. The first term describes the electron hopping; the hopping integral $t=1$ will be used in the following as the unit of energy. The second term describes the Coulomb repulsion for the e_g electrons; we will treat $U=0$ and $U=10$. The third term describes the ferromagnetic Hund's rule coupling between the e_g electrons and the t_{2g} core spins. In this work, we take $J_H=8$, which corresponds to $J_H=6$ in Refs. 19 and 2, if one compensates for the normalization of classical core spins to $|\vec{S}|=1$. The last term describes an additional direct superexchange between the core spins. For manganites, this effective interaction favors antiferromagnetic ordering of the core spins, i.e., $J'>0$. We vary J' from $J'=0$ to $J'=0.02$. Note that $J'=0.01$ corresponds to $J'=\frac{9}{4}\times 0.01 \approx 0.02$ in the units of Refs. 19 and 2.

We employ the density-matrix renormalization group, keeping up to 1000 states at each DMRG iteration and treating chains of length $L=24$ with open boundary conditions. The discarded weight is at most of order 10^{-6} for the results presented here. Our calculations indicate, however, that 48 states, as used in Ref. 6, would lead to insufficient accuracy for the system sizes treated here.

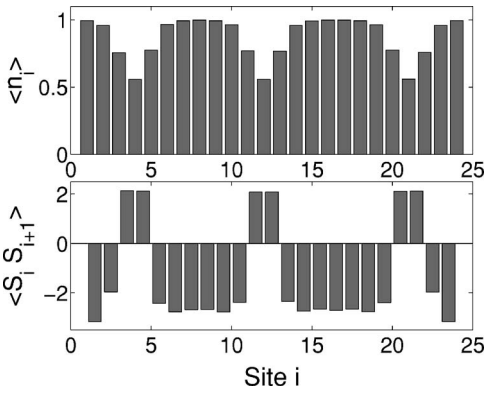

FIG. 1. Local density $\langle n_i\rangle$ and core spin-core spin correlations $\langle S_i S_{i+1}\rangle$ of the DMRG ground state for a chain of length $L=24$ with $J'=0.01$ and $U=0$. Three well-separated polarons can be clearly seen.

III. DMRG RESULTS

A. Ground-state configurations

1. Polarons are repulsive

Figure 1 shows the on-site electron density and the nearest-neighbor core spin correlation $\langle S_i S_{i+1}\rangle$ for a DMRG ground state for a chain of length $L=24$ for $J'=0.01$ and $U=0$ with three holes. The holes clearly form three individual polarons, each extending over approximately three sites with ferromagnetically aligned core spins that are embedded in an antiferromagnetic background.

Since the DMRG is a variational method, convergence to the true ground state is not guaranteed. Therefore, we have checked the consistency of the ground state by trying different system buildup strategies with respect to particle injection for many parameter sets. Thereby, we have examined whether there is degeneracy of states with respect to polaron positions and how far the existence of well-separated polarons and their positions are determined by the details of the DMRG algorithm. In addition, one can perform calculations with different z components S_z^{tot} of the total spin S^{tot}; increasing S_z^{tot} reduces the size of the Hilbert space. This, in general, allows for more accurate results, while the smaller Hilbert space still contains the ground state as long as $S_z^{\text{tot}} \leqslant S^{\text{tot}}$.

In an $L=24$ system with two holes ($J'=0.01, U=0$), we always find two polarons regardless of how the system is built up. All energies obtained are degenerate within the estimated numerical accuracy. The polaron position, however, depends on where the particles are injected. In all cases, we find polarons that are separated by at least a few lattice sites with AFM order. Even if we add both holes simultaneously during the system buildup, they separate into two polarons. Therefore, we conclude that well-separated polarons are effectively independent, while they seem to repel each other at short distances.

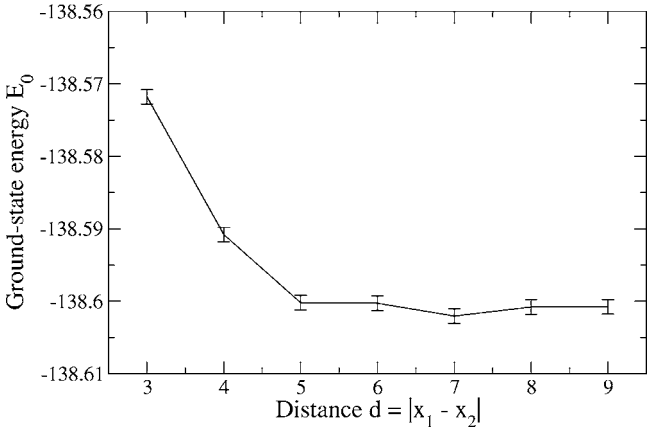

FIG. 2. Ground-state energy E_0 as a function of the distance d of two polarons on an $L=24$ site chain with $J'=0.01$, $U=0$. The holes are centered at the position of electrostatic impurity potentials $E_{\mathrm{pot}}=-0.1$ and exhibit a symmetric density distribution. The energies for $d\geqslant 5$ are degenerate within the estimated numerical accuracy as designated by the error bars.

We estimate the energy connected to this repulsion by introducing small electrostatic potentials $E_{\mathrm{pot}}=-0.1$ in order to trap the holes at sites x_1 and x_2. For all distances $d=|x_2-x_1|\geqslant 3$, we obtain FM polarons covering three lattice sites with on-site densities symmetric with respect to x_1 and x_2. The ground-state energy as a function of the distance $d=|x_2-x_1|$ is shown in Fig. 2, which corroborates the fact that polarons separated by two or more sites are effectively independent. The configuration with only one intermediate site is $\Delta E\approx 0.01$ higher in energy, and in order to obtain a state with adjacent polarons $\Delta E\approx 0.03$ has to be paid.

We therefore conclude that the holes actually have a *repulsive* interaction at short range and that separated polarons are energetically favored over phase separation into larger FM and AFM regions near the half-filled Kondo band for $J'=0.01$ and $U=0$.

The fact that we can obtain degenerate states with a localized polaron at different positions upon doping with one hole suggests that polarons are quasiparticles having a large effective mass. For physical reasons, we would expect that a single polaron delocalizes, forming a heavy Fermi liquid, but it appears that polarons have a bandwidth that is too small to be resolved by the DMRG.

2. Influence of J' and U and comparison to classical spins

In Ref. 2, the energy for phase separation was compared to that for independent polarons as a function of an effective superexchange J_{eff} of classical core spins for the almost-filled lower Kondo band ($n\lesssim 1$). At small values of J_{eff}, an increase in the optimal polaron size was found and bipolarons and phase separation dominated. The effective exchange J_{eff} is defined in terms of the t_{2g} superexchange J' and the energy $\varepsilon_{\mathrm{ex}}$ for virtual excitations into the upper Kondo band

$$J_{\mathrm{eff}}\approx J'+\frac{t^2}{\varepsilon_{\mathrm{ex}}}. \tag{2}$$

Without Coulomb repulsion, $\varepsilon_{\mathrm{ex}}$ is given by the energy for the low-spin state ^3E.[20] For finite Hubbard U, the energy for the virtual excitations is higher, however, because they lead to doubly occupied sites for $n\approx 1$; $\varepsilon_{\mathrm{ex}}$ is then given by the energetically higher ^4E and $^4A_2$ states.[21] Taking into account Coulomb repulsion should therefore have an effect similar to reducing J'.

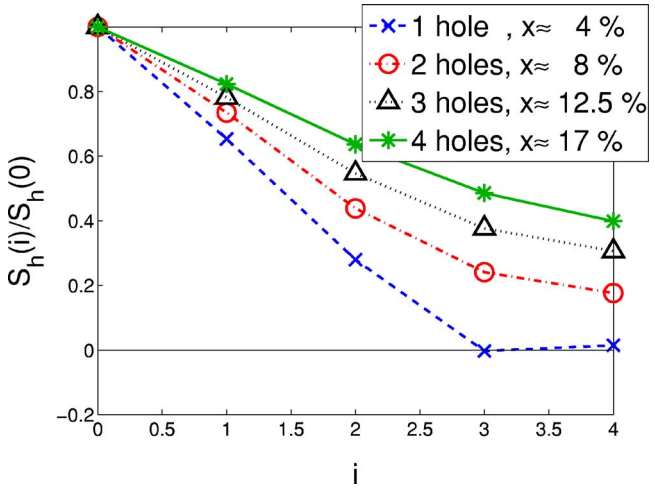

FIG. 3. (Color online) Dressed core spin correlation function, Eq. (3), for classical core spins with effective spinless fermions for $J'=0$, $U=0$, inverse temperature $\beta=1/T=100$, and an $L=24$ site chain. The ferromagnetic area grows with doping, indicating phase separation.

The spinless fermion model with classical core spins[19] forms polarons for $J'=0.01$ (corresponding to $J'\approx 0.02$ in the units of Ref. 2), but for $J'=0$, the polarons tend to attract each other and phase separate. This can be seen by examining the dressed core spin correlation function

$$S_h(r)=\frac{1}{L-r}\sum_{i=1}^{L-r} n_i^h S_i S_{i+r}, \tag{3}$$

where $n_i^h=(1-n_{i\uparrow})(1-n_{i\downarrow})$ gives the hole density relative to the half-filled chain, i.e., it is only nonzero if the site is unoccupied. We have evaluated this observable for the classical model with $J'=0$. The result, depicted in Fig. 3, shows that the ferromagnetic regions around the holes grow with doping (i.e., that the polarons attract each other and tend to phase separate).

The dressed core spin correlation function $S_h(r)$ is shown for quantum-mechanical core spins and $U=0$ in Fig. 4. For $J'=0.01$ the size of the ferromagnetic regions around the holes does not grow with doping in accordance with our analysis in Sec. III A 1. In the case of $J'=0$, we observe phase separation also for the quantum model, which is reflected in the pronounced increase of FM correlations with doping in Fig. 4(b). Without an on-site Coulomb repulsion U, we find that the spinless fermion model[2] agrees qualitatively very well with the present DMRG results, confirming that localized $S=3/2$ spins are well approximated by classical spins.

If ones takes a closer look at the numerical values of the dressed core spin correlation function for both models, one has to keep in mind that states with double occupation have

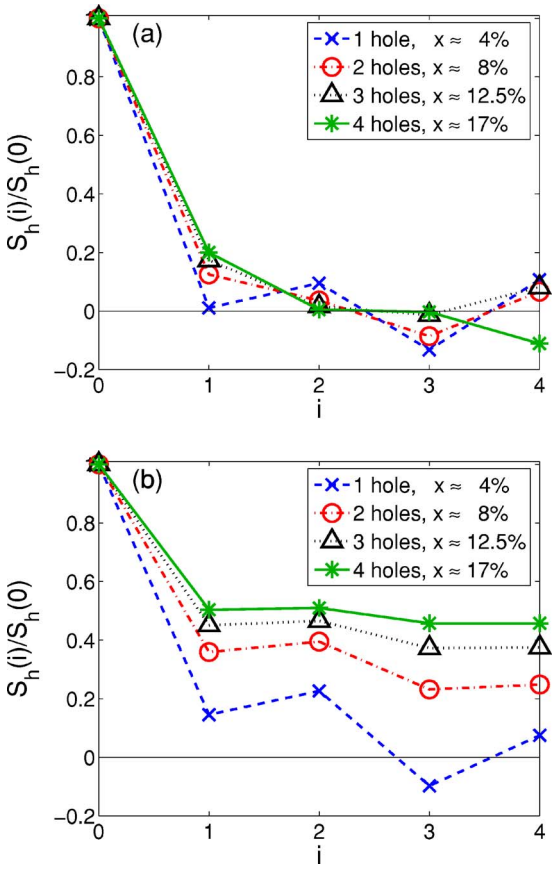

FIG. 4. (Color online) Dressed core spin correlation, Eq. (3), for quantum-mechanical core spins for $U=0$ and (a) $J'=0.01$ and (b) $J'=0$ on an $L=24$ site chain. In the polaronic regime (a), there is no dependence of the size of the ferromagnetic area on doping, in contrast to the phase separated case (b).

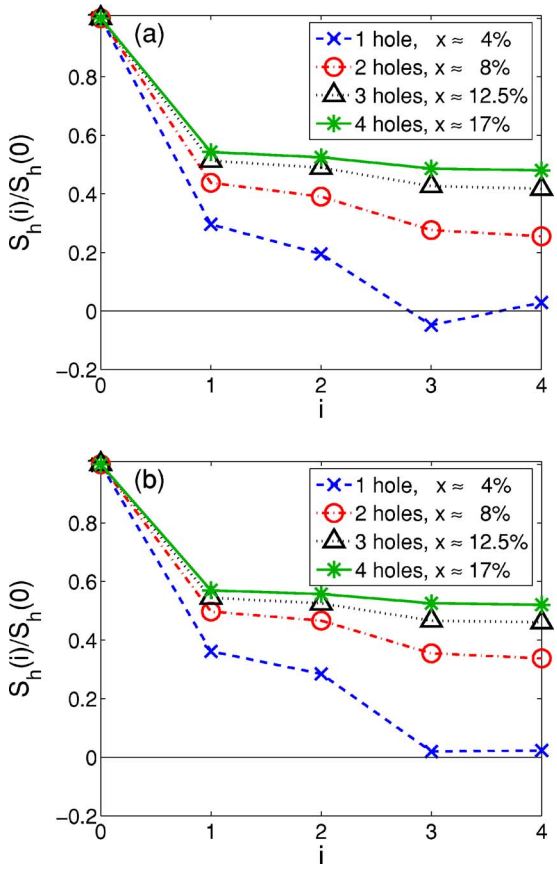

FIG. 5. (Color online) Dressed core spin correlation, Eq. (3), for quantum-mechanical core spins for $U=10$ and (a) $J'=0.01$ and (b) $J'=0$ on an $L=24$ site chain. The pronounced dependence on doping indicates phase separation.

been projected out in the classical case, while such states are included in the DMRG calculations. In the latter case, there is a finite hole density $\langle n_i^h \rangle \approx 0.014$ at sites i within the AFM background far from polarons, and still higher hole densities can be observed in the proximity of polarons. These contributions of the AFM background to the dressed core spin correlation function (3) partly cancel the FM terms from within the polarons in the quantum model; this accounts for the almost vanishing nearest-neighbor correlation $S_h(1)/S_h(0) \approx 0$ for one hole shown in Fig. 4(a).

The inclusion of a finite Hubbard $U=10$ decreases the effective exchange J_{eff} as discussed above and therefore increases the tendency to phase separation. In fact, phase separation takes place even for $J'=0.01$, which is reflected in the dressed core spin correlations in Fig. 5.

3. Transition to the homogeneous ferromagnetic phase

We first examine the polaronic case $J'=0.01$ and $U=0$, where the polarons extend over approximately three sites. The ground state of an $L=24$ chain for $x=1/4$ (six holes) shown in Fig. 6(a) corresponds to a periodic arrangement of polarons, in agreement with the energy considerations of Sec. III A 1. Similar "island phases" have also been found for $S=1/2$ core spins at commensurate fillings.[16] They consist of small ferromagnetic islands that are aligned antiferromagnetically or have one antialigned spin between them. Adding one more hole, we find that the polaronic configuration is destroyed and a large FM region forms with two AFM-arranged spins at each end [see Fig. 6(b)]. This could be a sign of phase separation; but, much larger chains would have to be treated in order to clarify this issue. For dopings of $x=0.375$ (nine holes on an $L=24$ chain), we observe complete FM polarization.

When the core spin superexchange is increased to $J'=0.02$ (still neglecting Coulomb repulsion $U=0$), polaronic states become stabilized up to dopings of $x=1/3$ and we find another island phase of AFM-stacked polarons for eight holes [see Fig. 7(a)]. The result for nine holes in Fig. 7(b) suggests phase separation between an island phase and a FM region; however, chains of length $L=24$ are too small to make definitive statements. As the treatment of much larger systems is not feasible using currently available computational resources and the main focus of this paper is the almost-filled lower Kondo band, we did not investigate the nature of the phase transition further. We finally note that upon doping the $L=24$ chain with ten or more holes, complete FM polarization is obtained (not shown).

For parameters $J'=0.02$ and $U=10$, the polaronic regime extents up to $x=1/4$ (6 holes), so the transition to ferromagnetism is very similar to the one obtained for $J'=0.01$ and

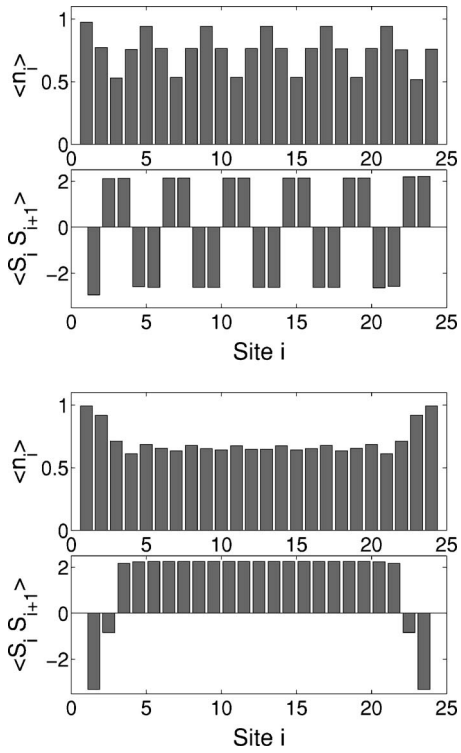

FIG. 6. On-site density $\langle n_i \rangle$ and core spin-core spin correlations $\langle S_i S_{i+1} \rangle$ of the DMRG ground state for $J'=0.01$, $U=0$ and (a) 6 holes ($x=1/4$) and (b) 7 holes.

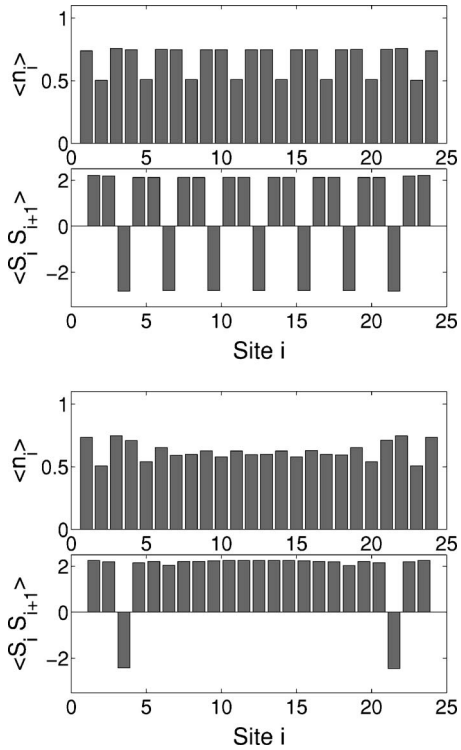

FIG. 7. On-site density $\langle n_i \rangle$ and core spin-core spin correlations $\langle S_i S_{i+1} \rangle$ of the DMRG ground state for $J'=0.02$, $U=0$ and (a) 8 holes ($x=1/3$) and (b) 9 holes.

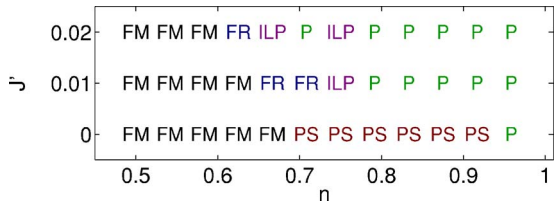

FIG. 8. (Color online) Phase diagram in the $n-J'$ plane for $U=0$. The symbols designate the following characteristics: P, polarons, ILP, island phase (periodic arrangement of polarons); PS, phase separation; FM, ferromagnetic; and FR, central ferromagnetic region with antiferromagnetically oriented sites at the ends of the chain. The symbols (letters) are determined for an $L=24$ site chain.

$U=0$. We find an island phase as already shown in Fig. 6(a) and for seven holes a configuration similar to the one shown in Fig. 6(b). At dopings of eight holes ($x=1/3$) complete FM polarization is obtained for $J'=0.02$ and $U=10$.

B. Phase diagrams

We summarize the impact of the parameters J' and U in phase diagrams in the $n-J'$ plane, where $n=1-x$ designates the filling and J' refers to the t_{2g} superexchange. Figure 8 shows the phase diagram for an $L=24$-site chain without Coulomb repulsion, $U=0$. One sees a polaronic region (P) near the filled lower Kondo band, including periodic arrangement of polarons (island phase, denoted as ILP) for commensurate fillings. For large $J'>0.01$, this region extends to hole densities $x\approx 1/3$, while phase separation is found for vanishing $J'=0$.

Some of our results indicate that there might be phase separation for intermediate fillings between polaronic and FM phases at $J'>0$. However, much longer chains would be needed to clarify this issue; see also our discussion in Sec. III A 3. Corresponding states with a large central FM region and either some AFM sites or polarons at both ends [cf. Figs. 6(b) and 7(b)] have been designated as FR in the phase diagram. Regions are labeled FM if *all* nearest-neighbor spin correlations are positive.

For $U=0$ and $J'=0$, we find phase separation (PS): By varying the system buildup, we are able to obtain both polaronic configurations and states with a larger FM region embedded in an AFM background; for these parameters, the phase-separated states always have a lower energy.

Although we expect macroscopic polarization in the thermodynamic limit near the empty Kondo band, as also observed in 1D for the $t-t'-U$ model[22,23] and a Cu-O chain,[24] we did not investigate the extent of polarization for finite systems in detail. We note that saturation should not be expected for quantum spins in the thermodynamic limit according to Ref. 15.

Figure 9 shows the phase diagram for Coulomb repulsion $U=10$. Comparing to $U=0$, we see that the polaronic phase is suppressed at lower doping and phase separation takes place even for $J'=0.01$. This is consistent with the reduction in the effective parameter J_{eff} with increasing U. For parameters $J'=0.01$ and $U=10$, we find that two holes can gain $\Delta E\approx 0.008$, forming a bipolaron instead of two separated

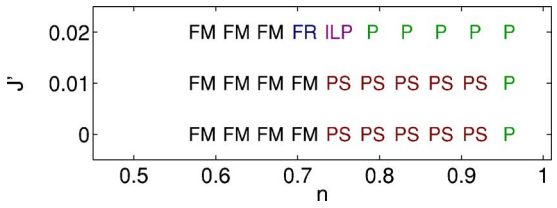

FIG. 9. (Color online) Phase diagram as in Fig. 8, but with $U=10$.

polarons. Compared to the energy $E\approx-137.318$ of the bipolaronic state, the energy difference is rather small and this is one reason for the sensitivity of the DMRG with respect to system buildup. If there are states very close in energy but far apart in phase space, numerical results will strongly depend on the initial configuration. We have designated the corresponding parts with PS in Fig. 9.

C. Compressibility

The inverse compressibility of a system can be computed approximately by numerical differentiation of energies by

$$\kappa^{-1}=\frac{N_e^2}{L}\frac{E(N_e+\Delta,L)+E(N_e-\Delta,L)-2E(N_e,L)}{\Delta^2}, \quad (4)$$

where $E(N_e,L)$ is the total energy of a chain with N_e electrons on L sites and Δ is the difference in particle number. Negative values are sometimes taken to be an indication of phase separation.[6]

We want to argue that this condition is neither necessary nor sufficient. On the one hand, negative values only result from finite-size effects and should vanish in the thermodynamic limit leading to $\kappa^{-1}\to 0$, as will be discussed below. On the other hand, we will show in Fig. 10 that polarons can cause $\kappa^{-1}\approx 0$ as well. Such observations therefore always have to be complemented by an investigation of correlation functions, e.g., the dressed core-spin correlation [Eq. (3)] in order to show the existence of two distinct phases.

First, we note that numerical methods, such as the DMRG or Monte Carlo calculations, which do not impose homogeneity, as, for instance, mean-field theory would, should yield separated phases in different spatial regions in a proportion that minimizes the free energy—in effect, the system performs the Maxwell construction by itself and should thus avoid negative compressibilities in the thermodynamic limit.

For phase separation on finite systems, however, negative compressibilities $\kappa^{-1}<0$ can indeed arise because the surface separating the two phases also contributes to the total energy. (From the occurrence of PS, it can be inferred that the phase boundary is not energetically favorable because the system would otherwise tend to *maximize* instead of minimizing it and form many small droplets or a mixed phase.) If this boundary has high-enough energy and grows with doping, its contribution to the total energy leads to a negative compressibility.

In the thermodynamic limit $L\to\infty$, such surface terms become negligible compared to the bulk contributions, implying $\kappa^{-1}\to 0$. Moreover, the boundary surface does not have

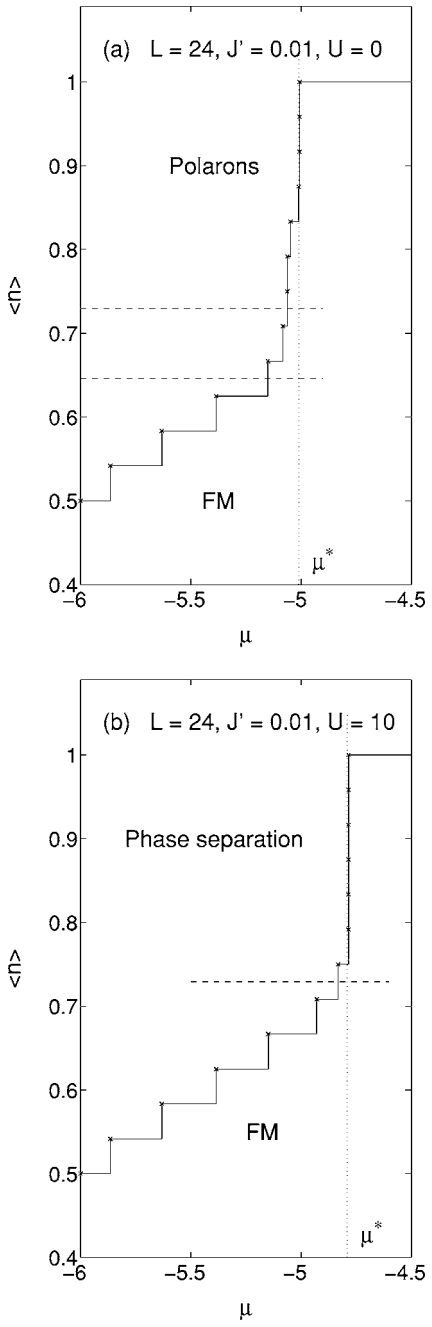

FIG. 10. Grand canonical expectation value for the electron density $\langle n\rangle$ vs chemical potential μ for $J'=0.01$, $L=24$ and (a) $U=0$, (b) $U=10$. The dashed lines indicate the limits of the (a) polaronic or (b) phase-separated and the FM regimes, respectively.

to grow with doping at all. In the present one-dimensional case, the phase boundary always consists of just two bonds connecting the two phases regardless of their size. For this reason, one could obtain $\kappa^{-1}\approx 0$ here even for finite systems. In addition, one has to keep in mind that numerical differentiation is notoriously sensitive to even small numerical errors of the ground-state energies entering Eq. (4).

A discontinuity of the density n as function of the chemical potential μ is equivalent to the limit of infinite compressibility $\kappa^{-1}\to 0$, and is likewise taken as an indication for phase separation. We will here show that it can arise from

independent polarons as well. In order to obtain $n(\mu)$ from the DMRG calculations at fixed particle numbers N_e, we set $n(\mu)=N_e/L$, where N_e minimizes the grand canonical expectation value $\langle \hat{H}-\mu\hat{N}\rangle = E(N_e,L)-\mu N_e$. The results for chains with $L=24$, $J'=0.01$, $U=0$ and $U=10$, respectively, are shown in Fig. 10.

We find a jump near $n\approx 1$ both for $U=10$, where PS is observed, as well as for $U=0$, where we see polarons. In the latter case, it can be accounted for by the independence of the polarons at low doping, i.e., adding each polaron costs the same energy, which is balanced by the chemical potential $\mu^* = \epsilon_{\mathrm{pol}}$.[2,7] This also corresponds to our observation that the ground-state energy per site as a function of filling (not shown) lies practically on an straight line near $n=1$ with $dE/dn=\epsilon_{\mathrm{pol}}$.

In conclusion, we have argued that a negative compressibility for a finite system is neither a necessary nor a sufficient condition for phase separation. It is also important to note that a discontinuity of the density n as function of the chemical potential μ is a necessary condition for phase separation, but is not a sufficient condition because other mechanisms, such as independent polarons, can induce a "jump" of $n(\mu)$ as well.

IV. CONCLUSIONS

We have presented an extensive numerical study of the one-dimensional ferromagnetic Kondo lattice model with quantum-mechanical $S=3/2$ core spins using the density-matrix renormalization group method, treating a nondegenerate conduction band with and without on-site Coulomb repulsion at low to intermediate doping. In particular, we have explored the similarities with the analogous model with classical core spins, where ferromagnetic polarons have been found to dominate over phase separation[2] for parameters relevant to manganites. We have investigated whether the inclusion of quantum fluctuations leads to an attractive interaction between the polarons and thus to phase separation. We find that this is not the case: the polarons are, in fact, *repulsive* at short distances. In general, the results of the quantum model agree very well with the classical model and show that classical spins are indeed a very good approximation for manganites.

Furthermore, we have investigated the influence of a relatively large local Coulomb repulsion $U=10$, which reduces the effective AFM coupling J_{eff} relevant when $n\lesssim 1$. For small t_{2g} superexchange $J'\leqslant 0.01$, phase separation dominates over separated polarons if on-site Coulomb repulsion is taken into account, while polarons are favored upon increasing the superexchange parameter to $J'=0.02$. We have summarized these findings in phase diagrams in the plane of doping and t_{2g} superexchange J' for $U=0$ and $U=10$.

We have also argued that the observation of a (small) negative compressibility and of a jump in the density n as a function of the chemical potential μ are not compelling indicators of phase separation. Although a discontinuity of $n(\mu)$ is a necessary condition for phase separation, it is not a sufficient one: different mechanisms, such as the formation of independent polarons, can leave similar traces.

ACKNOWLEDGMENT

This work has been supported by the Austrian Science Fund (FWF), Project No. P15834-PHY.

*Electronic address: neuber@itp.tu-graz.ac.at

[1] C. Zener, Phys. Rev. **82**, 403 (1951).
[2] W. Koller, A. Prüll, H. G. Evertz, and W. von der Linden, Phys. Rev. B **67**, 174418 (2003).
[3] E. Dagotto, T. Hotta, and A. Moreo, Phys. Rep. **344**, 1 (2001).
[4] N. Furukawa, in *Physics of Manganites*, edited by T. Kaplan and S. Mahanti (Kluwer Academic Publisher, Dordrecht, 1998).
[5] S. Yunoki, J. Hu, A. L. Malvezzi, A. Moreo, N. Furukawa, and E. Dagotto, Phys. Rev. Lett. **80**, 845 (1998).
[6] E. Dagotto, S. Yunoki, A. L. Malvezzi, A. Moreo, J. Hu, S. Capponi, D. Poilblanc, and N. Furukawa, Phys. Rev. B **58**, 6414 (1998).
[7] M. Daghofer, W. Koller, H. G. Evertz, and W. von der Linden, J. Phys.: Condens. Matter **16**, 1 (2004).
[8] C. D. Batista, J. M. Eroles, M. Avignon, and B. Alascio, Phys. Rev. B **58**, R14689 (1998).
[9] C. D. Batista, J. Eroles, M. Avignon, and B. Alascio, Phys. Rev. B **62**, 15047 (2000).
[10] G. Honner and M. Gulacsi, J. Supercond. **12**, 237 (1999).
[11] M. Yu Kagan, A. V. Klapstov, I. V. Brodsky, K. I. Kugel, A. O. Sboychakov, and A. L. Rakhmanov, J. Phys. A **36**, 9155 (2003).
[12] D. M. Edwards, Adv. Phys. **51**, 1259 (2002).
[13] D. Meyer, C. Santos, and W. Nolting, J. Phys.: Condens. Matter **13**, 2531 (2001).
[14] W. Müller and W. Nolting, Phys. Rev. B **66**, 085205 (2002).
[15] W. Nolting, G. G. Reddy, A. Ramakanth, D. Meyer, and J. Kienert, Phys. Rev. B **67**, 024426 (2003).
[16] D. J. Garcia, K. Hallberg, C. D. Batista, S. Capponi, D. Poilblanc, M. Avignon, and B. Alascio, Phys. Rev. B **65**, 134444 (2002).
[17] D. J. Garcia, K. Hallberg, C. D. Batista, M. Avignon, and B. Alascio, Phys. Rev. Lett. **85**, 3720 (2000).
[18] D. J. Garcia, K. Hallberg, B. Alascio, and M. Avignon, Phys. Rev. Lett. **93**, 177204 (2004).
[19] W. Koller, A. Prüll, H. G. Evertz, and W. von der Linden, Phys. Rev. B **66**, 144425 (2002).
[20] A. M. Oleś and L. F. Feiner, Phys. Rev. B **65**, 052414 (2002).
[21] L. F. Feiner and A. M. Oleś, Phys. Rev. B **59**, 3295 (1999).
[22] S. Daul and R. M. Noack, Phys. Rev. B **58**, 2635 (1998).
[23] S. Daul and R. M. Noack, Phys. Rev. B **61**, 1646 (2000).
[24] M. Guerrero and R. M. Noack, Phys. Rev. B **63**, 144423 (2001).